Available online at www.sciencedirect.com
SCIENCE DIRECT
European Journal of Mechanics B/Fluids 24 (2005) 205–218

Strong shock waves generated by a piston moving in a dust-laden gas under isothermal condition

Walter Gretler *, René Regenfelder

Technical University Graz, Inst. of Fluid Mechanics and Heat Transfer, Inffeldgasse 25/F, 8010 Graz, Austria

Received 17 June 2004; accepted 5 July 2004

Available online 17 September 2004

Abstract

The problem of strong shock-wave propagation through a dust-laden gas is studied as a limiting case of very intensive heat transfer. According to a potential law, the variable energy input is continuously supplied by a driving piston or a surface. A self-similar solution is found under isothermal condition of the flow field. The spherical case is worked out in detail to investigate to what extent the shock wave is influenced by the energy input as well as by the mass concentration of the solid particles in the medium and the ratio of density of the solid particles to the initial density of the medium. Three different cases are covered with respect to parameters describing the increase of energy or the piston velocity: One corresponds to a decelerated piston, the second to a constant piston velocity and the third to a continuously accelerated piston starting from rest. The dust-free flow is included in the numerical results as a limiting case.

Keywords: Strong shock waves; Dusty gas; Isothermal flow; Self-similar solution

1. Introduction

Similarity solutions for planar radiating shock waves driven by a piston in a dust-free gas were first obtained by Wang [1], accounting for radiation diffusion or radiation losses in optically thick and thin limits, respectively. Radiating shock waves driven by a piston in a dust-free gas for planar, cylindrical and spherical geometry were discussed by Helliwell [2]. When intense heat exchange between particles of gas takes place, we may assume that there is no temperature gradient throughout the flow field, i.e., $\partial T/\partial r \to 0$. Therefore, the temperature in the flow field depends only on time t and not on the distance r from the center of the explosion, i.e., $T = T(t)$, and the flow is isothermal. This assumption on the character of the flow corresponds to the beginning of a very strong explosion (for example: coal-mine blasts, underground, volcanic and cosmic explosions) when the gas temperature is extremely high. Solutions for such self-similar flows for particle-free gas were studied by Korobeinikov [3], Laumbach and Probstein [4], Narasimhulu Naidu et al. [5] and Levin and Zhuravskaya [6]. An approximate analytical solution was obtained by Narasimhulu Naidu et al. [7] for self-similar flow behind a strong shock wave in a dust-laden gas with variable energy release, whereas in our previous paper [8] the exact numerical solution for this problem was presented.

* Corresponding author. Tel.: +43-316-873-7348; fax: +43-316-873-7848.
E-mail address: gretler@tugraz.at (W. Gretler).

0997-7546/$ – see front matter
doi:10.1016/j.euromechflu.2004.07.001

Nomenclature

Latin symbols

a_a	sound speed ahead of the shock front
a_{isoth}	isothermal-sound speed of the mixture
c	proportionality constant
c_{sp}	specific heat of the solid particles
c_v	specific heat of the gas at constant volume
c_{pm}	specific heat of the mixture at constant pressure
c_{vm}	specific heat of the mixture at constant volume
e	specific internal energy of the mixture
f	non-dimensional velocity
F	reduced flow velocity
g	non-dimensional pressure
G	ratio of the density of solid particles to that of the perfect gas at the initial state
h	non-dimensional density
j	geometry factor
J	energy integral
k_p	mass fraction (concentration) of the solid particles
M	shock Mach number
m	total mass of the mixture
m_{sp}	total mass of the solid particles
n_j	geometrical factor
P	proportionality constant and singular points, respectively
q	total heat flux
Q	total non-dimensional heat flux
r	space coordinate
R_i	gas constant
t	time coordinate
T	absolute temperature of the mixture
u	flow velocity
V	volume of the mixture
V_a	volume of the mixture at the initial state
V_{sp}	volumetric extension of the solid particles
W_n	shock-propagation velocity
x	field coordinate (similarity variable)
y	front coordinate (reciprocal square of Mach number)
Y	reduced isothermal sound speed of the mixture
Z	volume fraction of the solid particles

Greek symbols

α	proportionality constant
β_{sp}	ratio of specific heats of the solid particles
γ	ratio of specific heats of the gas
Γ	ratio of specific heats of the mixture
δ	abbreviation
Θ	non-dimensional temperature
λ	decay coefficient of the front velocity
Ψ	function of f and h
ϱ	density of the mixture
ϱ_g	density of the gas
ϱ_{sp}	density of the solid particles
σ_n	non-dimensional internal energy deposited at the front
τ	compressibility

Subscripts

a	conditions immediately in front of the shock
isoth	isothermal
n	conditions immediately behind the shock front
m	mixture
p	piston, constant pressure
v	constant volume
0, 1, 2, 3, 4, 5	signifies singular points in the (F, Y)-plane

In the present paper the piston problem of shock-wave propagation in a dust-laden gas under isothermal condition is investigated by assuming that the solid particles behave like a pseudo-fluid. Following Pai [9], we treat the isothermal flow as a mixture of a gas and a pseudo-fluid at a velocity and temperature equilibrium with a constant ratio of specific heat of the mixture. For this gas-particle mixture to be treated as a so-called idealized equilibrium gas [10], it is necessary to consider the particle diameter much smaller than a characteristic length of the flow field. Applying the similarity requirements, the governing equations result in a boundary value problem consisting of three ordinary differential equations in which the dimensionless temperature Θ appears as a constant parameter. The calculations are performed in the case of spherical symmetry for different values of mass concentrations of the solid particles and for the density ratio of solid particles to the initial density of the gas. Results for a number of representative cases are listed in tables and illustrated in terms of integral curves in the phase plane of reduced variables as well as in the form of velocity, density, pressure and heat flux profiles across the flow field.

2. Basic equations

The velocity component in the radial direction u, material density ϱ and pressure p are functions of time t and radial coordinate r, while j denotes a geometry factor; $j = 0, 1$ or 2 characterizes flows with plane, cylindrical or spherical symmetry.

As mentioned above the temperature T in the flow field between the shock wave and the piston surface is only a function of time t. The conservation equations governing the dusty-gas flow can be expressed as

$$\frac{\partial \varrho}{\partial t} + u\frac{\partial \varrho}{\partial r} + \varrho\frac{\partial u}{\partial r} = -j\frac{\varrho u}{r}, \tag{1}$$

$$\frac{\partial u}{\partial t} + u\frac{\partial u}{\partial r} + \frac{R_i T(1-k_p)}{\varrho(1-Z)^2}\frac{\partial \varrho}{\partial r} = 0, \tag{2}$$

$$\frac{\partial T}{\partial r} = 0, \tag{3}$$

where $(\partial p/\partial \varrho)_T = p/[\varrho(1-Z)]$ expressing the isothermal sound speed

$$a^2_{\text{isoth}} = \frac{R_i T(1-k_p)}{(1-Z)^2} \tag{4}$$

is replaced with the equation of state of the mixture under equilibrium condition

$$p = \left(\frac{1-k_p}{1-Z}\right)\varrho R_i T. \tag{5}$$

Here $k_p = m_{sp}/m$ is the mass fraction (concentration) of the solid particles in the mixture taken as a constant in the whole flow field and $Z = V_{sp}/V$, where m_{sp} and V_{sp} are the total mass and the volumetric extension of the solid particles, respectively. R_i is the specific gas constant of the dust-free (perfect) gas. The relation between the fractions k_p of the total mass m and Z of the volume V of the mixture is given by Pai et al. [9]. Accordingly, $k_p = (Z\varrho_{sp})/\varrho$ where $Z = (Z_a/\varrho_a)\varrho$, while ϱ_{sp} is the species density of the solid particles and subscript a refers to the initial values of Z and ϱ. For Z_a, we have the formula

$$Z_a = \frac{V_{sp}}{V_a} = \frac{k_p}{G(1-k_p)+k_p}, \tag{6}$$

where $G = \varrho_{sp}/\varrho_{ga}$ is the ratio of density of the solid particles to the initial density of the gas. The deviation of the behavior of a dusty gas from that of a perfect gas is indicated in Eq. (2) by the isothermal compressibility

$$\tau = \frac{1}{\varrho a^2_{\text{isoth}}}. \tag{7}$$

The volumetric fraction of the dust lowers the compressibility of the mixture, while the mass of the solid particles increases the total mass, and therefore may add to the inertia of the mixture. This can be demonstrated in two limiting cases of the mixture at the initial state. For $G = 1$, it follows from Eqs. (6), (5) and (7) that $Z_a = k_p$, $\varrho_a = p_a/R_i T$ and $\tau = (1-k_p)/p_a$, i.e., the presence of the solid particles linearly lowers the compressibility of the mixture in the initial state. In the other limiting case, i.e., for $G \to \infty$, the volumetric extension of the solid particles V_{sp} tends to zero. According to Eq. (6), the volumetric fraction Z_a is equal to zero. In this case, the compressibility $\tau = 1/p_a$ is not effected by the dust. The solid particles contribute only to increasing the mass and inertia of the mixture.

The ratio of the specific heats of the mixture is given by

$$\Gamma = c_{pm}/c_{vm} = (\gamma + \delta\beta_{sp})/(1+\delta\beta_{sp}), \tag{8}$$

where $\gamma = c_p/c_v$ is the specific heat ratio of the gas, $\beta_{sp} = c_{sp}/c_v$ is the specific heat ratio of the solid particles and δ is the abbreviation $\delta = k_p/(1-k_p)$.

In order to transform the governing Eqs. (1)–(3) into a system of dimensionless partial differential equations, we introduce the following dimensionless variables together with the shock decay parameter λ which expresses the deceleration of the wave front (W_n and a_a are the shock-propagation velocity and the sound speed ahead of the shock front, respectively):

$$x = \frac{r}{r_n}, \quad y = \frac{a_a^2}{W_n^2} = \frac{1}{M^2}, \quad f \equiv \frac{u}{W_n}, \quad g \equiv \frac{p}{\varrho_a W_n^2},$$
$$h \equiv \frac{\varrho}{\varrho_a}, \quad Q \equiv \frac{q}{\varrho_a W_n^3}, \quad \Theta \equiv (1-k_p)\frac{R_i T}{W_n^2} = (1-Z)\frac{g}{h}, \quad \sigma \equiv \frac{e}{W_n^2}, \tag{9}$$

$$\lambda = -2\frac{\partial(\ln W_n)}{\partial(\ln r_n)}, \tag{10}$$

where x and y refer to the field coordinate (or the similarity variable) and to the front coordinate, while the subscripts a and n refer to the values of the undisturbed medium and shock front, respectively. Further q is the heat flux and e is the internal energy.

The governing equations can now be written in the following non-dimensional form:

$$\lambda y\frac{\partial h}{\partial y}+(f-x)\frac{\partial h}{\partial x}+h\left(\frac{\partial f}{\partial x}+j\frac{f}{x}\right)=0, \tag{11}$$

$$\lambda y\frac{\partial f}{\partial y}+(f-x)\frac{\partial f}{\partial x}-\frac{\lambda}{2}f+\frac{\Theta}{h(1-Z)^2}\frac{\partial h}{\partial x}=0, \tag{12}$$

$$\frac{\partial \Theta}{\partial x}=0. \tag{13}$$

In the strong shock limit, in which the counter-pressure effects may be ignored, y tends to zero in the transformed system of equations yielding the following system of equations depending only on x (details of the computation can be found in a previous paper (Gretler and Regenfelder [12]):

$$\frac{\mathrm{d}h}{\mathrm{d}x}=\frac{(1-Z)^2}{\Theta}\left(\frac{\lambda}{2}fh-h(f-x)\frac{\mathrm{d}f}{\mathrm{d}x}\right), \tag{14}$$

$$\frac{\mathrm{d}f}{\mathrm{d}x}=\frac{(1-Z)^2(\lambda/2)f(f-x)+j(f/x)\Theta}{(1-Z)^2(f-x)^2-\Theta}, \tag{15}$$

$$\frac{\mathrm{d}Q}{\mathrm{d}x}=-j\frac{Q}{x}+\frac{\Theta h}{\Gamma-1}\left(\lambda-\frac{\Gamma}{1-Z}\left(j\frac{f}{x}+\frac{\mathrm{d}f}{\mathrm{d}x}\right)-\frac{(f-x)}{(1-Z)h}\frac{\mathrm{d}h}{\mathrm{d}x}\right). \tag{16}$$

The boundary conditions at the piston can be written as

$$f(x_p)=x_p,\qquad Q(x_p)=0 \tag{17}$$

and at the shock front as

$$h_n=\frac{1}{1-f_n}, \tag{18}$$

$$g_n=f_n+\frac{1-Z_a}{\Gamma}y, \tag{19}$$

$$\sigma_n=Q_n+\frac{f_n^2}{2}+\frac{1-Z_a}{\Gamma}y\left(f_n+\frac{1-Z_a}{\Gamma-1}\right), \tag{20}$$

$$f_n=\frac{1}{2}(1-Z_a)\left(1-\frac{y}{\Gamma}\right)+\frac{1}{2}\sqrt{(1-Z_a)^2\left(1+\frac{y}{\Gamma}\right)^2-4\Theta}. \tag{21}$$

According to Eqs. (14) and (18), the temperature is rendered uniform by radiation transport of energy Q. The maximum of heat flux Q_n is anticipated at the shock front. If we assume $y=0$ in Eqs. (17), (18) and (19), they are reduced to the boundary conditions in the strong shock limit:

$$f_n=\frac{1}{2}(1-Z_a)+\frac{1}{2}\sqrt{(1-Z_a)^2-4\Theta}, \tag{22}$$

$$h_n=\frac{2}{1+Z_a-\sqrt{(1-Z_a)^2-4\Theta}}, \tag{23}$$

$$\sigma_n=\frac{e_n}{W_n^2}=\left(\frac{1-Z_ah_n}{\Gamma-1}\right)\frac{g_n}{h_n}. \tag{24}$$

However, from these equations, it follows that in cases ($n=0$, $y>0$) and ($n\neq 0$, $y=0$) the conditions $(1-Z_a)(1+y/\Gamma)\geqslant 2\sqrt{\Theta}$ and $1-Z_a\geqslant 2\sqrt{\Theta}$, respectively, must be satisfied. Hence, it becomes obvious from Eq. (6) that G cannot be reduced arbitrarily for a fixed k_p.

Integrating Eq. (14) from x to $x=1$, we obtain

$$h=\frac{h_n\exp\Psi(f,h)}{1-Z_ah_n(1-\exp\Psi(f,h))}, \tag{25}$$

where

$$\Psi=\frac{1}{\Theta}\left(-\frac{1}{2}f^2+xf+\left(\frac{\lambda}{2}-1\right)\int_1^x f\,\mathrm{d}x+\frac{1}{2}f_n^2-f_n\right)+\frac{Z_a(h_n-h)}{(1-Z_ah_n)(1-Z_ah)}. \tag{26}$$

Thus the isothermal solution reduces essentially to finding the function $f(x)$ from Eqs. (15) and (25). If $Z_a = 0$, we obtain f as a solution of the Cauchy problem $\mathrm{d}f/\mathrm{d}x = \text{function}(x, f, \Theta, \lambda)$; $f(1) = f_n$. This solution describes two limiting cases, namely the case of infinite G at $k_p > 0$ when the initial density of the gas approaches zero and the dust-free case of $k_p = 0$. It is interesting to note that the dust-laden solution for $G = \infty$ can be obtained from the dust-free solution if γ is replaced by Γ (Eq. (8)). Apart from these limiting cases, this solution way provide no advantage in the general dust-laden case ($Z_a > 0$ at finite G), but it is suitable to check the results which are found by solving the system of Eqs. (14), (15) in the usual manner of Runge–Kutta technique. It should be emphasized that for isothermal flow, the dimensionless functions f and h do not depend on Γ, as follows from Eqs. (14), (15) and the boundary conditions Eqs. (22), (23) and (17). The effect of Γ appears only in the equations considering the energy balance, i.e., Eqs. (30) and (16).

Eqs. (17) and (20) state that the material receives no radiation from the piston and that heat losses from the shock front are negligible; in other words, we regard the shock front as opaque and the piston surface as black and cool. Therefore, the total energy of the system which is increasing with time according to a power law (Freeman [11])

$$\int_{r_p}^{r_n} \left(e + \frac{u^2}{2}\right) \varrho r^j \,\mathrm{d}r = \int_0^{r_n} e_a \varrho_a r^j \,\mathrm{d}r + \frac{P}{n_j} t^\beta \tag{27}$$

can be expressed in non-dimensional form for self-similar solution:

$$J = \frac{(n+1)^{j+1}\alpha^{j+3}}{n_j} \frac{P}{\varrho_a c^{j+3}}, \tag{28}$$

$$J = \frac{P\alpha^{j+3}}{\varrho_a c^{j+3} n_j} + \frac{y(1-Z_a)^2}{\Gamma(\Gamma-1)(j+1)} \quad (n = 0,\ y > 0), \tag{29}$$

where for similarity requirements $n + 1 = 2/(\lambda + 2)$ and $n = (\beta - j - 1)/(j + 3)$. Here J is defined by

$$J = \int_\alpha^1 h\left(\frac{1 - Z_a h}{\Gamma - 1}\frac{g}{h} + \frac{f^2}{2}\right) x^j \,\mathrm{d}x. \tag{30}$$

On the other hand, for self-similar flow, the work done by the piston can be described by the same power law

$$n_j \int_0^t p_p u_p r_p^j \,\mathrm{d}t = P t^\beta. \tag{31}$$

To perform the integration, we use Eq. (9) and the piston condition equation (17) with $W_n = ct^n/\alpha$, $u_p = \alpha W_n$ and $r_n = ct^{n+1}/(n+1)\alpha$, thus obtaining

$$P = \frac{n_j \varrho_a c^{j+3} g_p}{\alpha^2 \beta (n+1)^j}. \tag{32}$$

Substituting this for P in Eqs. (28) and (29), we get

$$J = \frac{1}{\beta}(n+1)\alpha^{j+1} g_p, \tag{33}$$

$$J = \frac{\alpha^{j+1} g_p}{j+1} + \frac{y(1-Z_a)^2}{\Gamma(\Gamma-1)(j+1)} \quad (n = 0,\ y > 0). \tag{34}$$

Using the new variables

$$F = \frac{f}{x}, \qquad Y = \frac{\Theta}{x^2(1-Z)^2}, \tag{35}$$

Eq. (15) can be transformed into

$$\frac{\mathrm{d}Y}{\mathrm{d}F} = \frac{2Y[(1-Z)(Y-(1-F)^2) + ZF((1-F)j - \lambda/2)]}{(1-Z)F[(j+1)Y - (1-F)(1-F+\lambda/2)]}, \tag{36}$$

or for $G = \infty$ ($Z = 0$ and $k_p > 0$)

$$\frac{\mathrm{d}Y}{\mathrm{d}F} = \frac{2Y[Y-(1-F)^2]}{F[(j+1)Y - (1-F)(1-F+\lambda/2)]}. \tag{37}$$

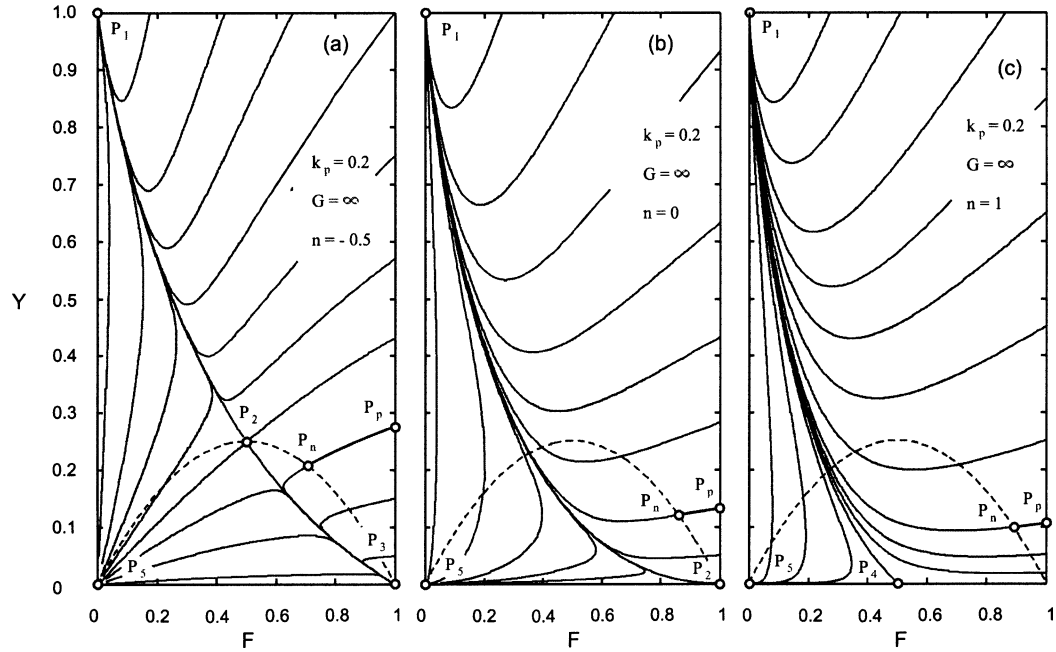

Fig. 1. The integral curves in the phase plane for spherical flow of a dust-laden gas under isothermal condition in the limiting case $G = \infty$, $k_p = 0.2$ presented in (a) for $n = -0.5$, in (b) for $n = 0$ and in (c) for $n = 1$. The singular points P_1–P_5 as well as the shock points P_n and the piston points P_p are indicated by small circles.

In order to study the behavior of the solution of Eq. (37), we consider the field of integral curves which are shown in Fig. 1.

Note that in the conventional phase plane Eq. (37) has the following singular points:

$$P_0(0,\infty), \quad P_1(0,1), \quad P_2(1-\lambda/2j, \lambda^2/4j^2),$$
$$P_3(1,0), \quad P_4(1+\lambda/2,0), \quad P_5(0,0), \tag{38}$$

where Y becomes infinite as x approaches zero or where both numerator and denominator become simultaneously equal to zero. Fortunately, all these singularities are located outside the range of interest in the (F, Y)-plane, which extends from the shock point P_n to the piston path P_p without crossing a limiting characteristic (acoustic line), i.e.:

$$\frac{1}{2}(1-Z_a) + \frac{1}{2}\sqrt{(1-Z_a)^2 - 4\Theta} \leqslant F \leqslant 1, \quad Y > 0. \tag{39}$$

The corresponding integral curves for $Z = 0$ and $G = \infty$ are represented on Fig. 1 by lines P_n–P_p. In this range the flow is subsonic, since

$$Y - (1-F)^2 > 0, \quad \text{or} \quad F \pm \sqrt{Y} > 1. \tag{40}$$

For the case $n = 0$, the Rankine–Hugoniot curve in the phase plane is given by a relation (obtainable from Eqs. (35), (9), (18) and (19) at $x = 1$) as follows:

$$Y_n = \frac{(F_n + ((1-Z_a)/\Gamma)y)(1-F_n)^2}{1-F_n-Z_a}. \tag{41}$$

For cases $n > -1$ and $n > 0$ where $y = 0$, Eq. (41) reduces to

$$Y_n = \frac{F_n(1-F_n)^2}{1-F_n-Z_a}. \tag{42}$$

This relation is displayed on Fig. 1 by broken lines.

3. Results

The set of ordinary differential equations, Eqs. (14)–(16), is solved simultaneously, using the Runge–Kutta fourth order method with a step size of $\Delta x = 10^{-4}$. The integration is carried out from the piston surface where $x_p = f_p$ and proceeds outward to the shock front ($x = 1$). Since, however, x_p is not known prior to the integration, the method of trial and error is applied starting with guessed values of Θ, g_p and x_p. Afterwards we checked the solution accuracy, using Eqs. (25) and (26) with known values of $f(x)$ and $h(x)$ in the interval $(x_p, 1)$.

Values of f, g, h and Q at both piston and shock front as well as values of Ψ and Θ, evaluated for $n = -0.5$, $n = 1$ and $y = 0$ are listed in Table 1, while such for $n = 0$, $y = 0$ and $y = 0.01$ are listed in Table 2. It may be noticed that the effects of the dusty gas enter through the parameter k_p, G and β_{sp}. These values are evaluated for $G = 0, 1, 10, 100, 1000$ and $k_p = 0, 0.1, 0.2, 0.3, 0.4$ at $\beta_{sp} = 1$ in order to exhibit some of the features of the dust-laden flow or a deviation from the dust-free flow. For example, an increase of any of the parameter k_p or G causes the dimensionless temperature Θ to decrease owning to the presence of the gas particles.

Moreover, the values of the energy integral for the isothermal flow are compared in Figs. 2, 3 and 4 with those for adiabatic flow. In the case $n = -0.5$ Fig. 2 shows that the presented values of the energy integral for both isothermal and adiabatic flow decrease for $G = 1$ with increasing k_p and increase for $G \geqslant 10$ with increasing k_p. This lies in the fact that for $G \geqslant 10$ the

Table 1
Dimensionless variables f, g, h, Q, Θ and function Ψ at the boundaries for spherical flow of a dust-laden gas under isothermal condition in cases $n \neq 0$ for different values of G and k_p; $\gamma = 1.4$

G	k_p	f_p	g_p	h_p	f_n	h_n	Q_n	Θ	Ψ_p
$n = -0.5$									
0	0	0.8466	0.4537	2.0279	0.6621	2.9597	0.3401	0.2237	−0.37808
1	0.1	0.8292	0.4295	1.9516	0.6093	2.5596	0.3064	0.1771	−0.34977
	0.2	0.8092	0.4035	1.8649	0.5560	2.2522	0.2694	0.1357	−0.32059
	0.3	0.7862	0.3753	1.7690	0.5015	2.0059	0.2298	0.0996	−0.28980
	0.4	0.7590	0.3444	1.6658	0.4450	1.8016	0.1885	0.0690	−0.25622
10	0.1	0.8540	0.4625	2.1297	0.6746	3.0732	0.3616	0.2121	−0.37741
	0.2	0.8614	0.4713	2.2458	0.6867	3.1923	0.3841	0.1984	−0.37641
	0.3	0.8685	0.4797	2.3766	0.6979	3.3105	0.4069	0.1821	−0.37257
	0.4	0.8748	0.4872	2.5195	0.7071	3.4142	0.4288	0.1629	−0.37257
100	0.1	0.8567	0.4662	2.1514	0.6819	3.1433	0.3680	0.2162	−0.38027
	0.2	0.8674	0.4797	2.3041	0.7031	3.3684	0.3996	0.2070	−0.38244
	0.3	0.8789	0.4943	2.4975	0.7261	3.6505	0.4357	0.1958	−0.38457
	0.4	0.8910	0.5101	2.7499	0.7508	4.0134	0.4769	0.1821	−0.38664
1000	0.1	0.8570	0.4665	2.1536	0.6826	3.1506	0.3686	0.2166	−0.38056
	0.2	0.8680	0.4805	2.3102	0.7048	3.3876	0.4012	0.2079	−0.38305
	0.3	0.8799	0.4958	2.5107	0.7290	3.6900	0.4387	0.1972	−0.3855
	0.4	0.8927	0.5125	2.7769	0.7555	4.0900	0.4822	0.1842	−0.38808
$n = 1$									
0	0	0.9584	1.0758	9.2323	0.8653	7.4265	−0.0831	0.1165	0.21765
1	0.1	0.9297	1.0178	5.3791	0.7892	4.7443	−0.0686	0.0874	0.25431
	0.2	0.8981	0.9662	3.7582	0.7111	3.4619	−0.0554	0.0632	0.29609
	0.3	0.8630	0.8904	2.8660	0.6310	2.7098	−0.0435	0.0436	0.34446
	0.4	0.8235	0.8197	2.3020	0.5486	2.2152	−0.0329	0.0282	0.40161
10	0.1	0.9587	1.0768	9.2112	0.8680	7.5737	−0.0848	0.1051	0.21557
	0.2	0.9583	1.0762	9.0159	0.8684	7.5975	−0.0860	0.0931	0.21455
	0.3	0.9568	1.0733	8.6009	0.8657	7.4463	−0.0866	0.0807	0.21498
	0.4	0.9536	1.0671	7.9351	0.8585	7.0693	−0.0861	0.0678	0.21751
100	0.1	0.9619	1.0832	10.0000	0.8767	8.1107	−0.0868	0.1071	0.21152
	0.2	0.9653	1.0907	10.9107	0.8880	8.9285	−0.0904	0.0972	0.20556
	0.3	0.9687	1.0980	11.9938	0.8991	9.9133	−0.0940	0.0869	0.19982
	0.4	0.9719	1.1051	13.2721	0.9099	11.1001	−0.0975	0.0759	0.19436
1000	0.1	0.9622	1.0839	10.0873	0.8776	8.1693	−0.0870	0.1073	0.21111
	0.2	0.9660	1.0921	11.1507	0.8900	9.0917	−0.0908	0.0977	0.20465
	0.3	0.9699	1.1006	12.5077	0.9026	10.2680	−0.0948	0.0875	0.19828
	0.4	0.9738	1.1091	14.2961	0.9154	11.8185	−0.0988	0.0768	0.19828

Table 2
Dimensionless variables f, g, h, Q, Θ and function Ψ at the boundaries for spherical flow of a dust-laden gas under isothermal condition in case $n = 0$ for different values of y, G and k_p; $\gamma = 1.4$

y	G	k_p	f_p	g_p	h_p	f_n	h_n	Q_n	Θ	Ψ_p
0	0	0	0.9429	0.8889	6.3231	0.8308	5.9098	0.0063	0.1406	0.06760
	1	0.1	0.9161	0.8399	4.4102	0.7599	4.1650	0.0070	0.1065	0.10013
		0.2	0.8864	0.7878	3.3489	0.6869	3.1939	0.0069	0.0777	0.13710
		0.3	0.8531	0.7321	2.6748	0.6116	2.5745	0.0061	0.0541	0.17990
		0.4	0.8155	0.6721	2.2092	0.5337	2.1446	0.0050	0.0354	0.23053
	10	0.1	0.9445	0.8920	6.4816	0.8361	6.1026	0.0055	0.1278	0.06472
		0.2	0.9454	0.8939	6.5686	0.8395	6.2297	0.0048	0.1143	0.06278
		0.3	0.9453	0.8938	6.5406	0.8399	6.2478	0.0041	0.0999	0.06212
		0.4	0.9436	0.8908	6.3437	0.8361	6.1030	0.0035	0.0847	0.06331
	100	0.1	0.9475	0.8977	6.8369	0.8446	6.4351	0.0053	0.1303	0.06102
		0.2	0.9522	0.9067	7.4578	0.8585	7.0683	0.0043	0.1193	0.05462
		0.3	0.9570	0.9158	8.2169	0.8725	7.8415	0.0035	0.1075	0.04842
		0.4	0.9616	0.9247	9.1531	0.8863	8.7948	0.0027	0.0949	0.04247
	1000	0.1	0.9478	0.8983	6.8750	0.8455	6.4707	0.0053	0.1306	0.06065
		0.2	0.9529	0.9080	7.5626	0.8605	7.1672	0.0043	0.1198	0.05380
		0.3	0.9582	0.9180	8.4422	0.8759	8.0558	0.0034	0.1083	0.04702
		0.4	0.9635	0.9283	9.6060	0.8916	9.2287	0.0026	0.0960	0.04033
0.01		0	0.9399	0.8905	6.0377	0.8222	5.6230	0.0070	0.1475	0.0712
	1	0.1	0.9132	0.8414	4.2836	0.7520	4.0321	0.0076	0.1123	0.1036
		0.2	0.8837	0.7892	3.2840	0.6797	3.1224	0.0074	0.0825	0.1404
		0.3	0.8506	0.7333	2.6388	0.6052	2.5329	0.0067	0.0579	0.1830
		0.4	0.8131	0.6731	2.1886	0.5281	2.1193	0.0055	0.0383	0.2334
	10	0.1	0.9415	0.8937	6.1788	0.8275	5.7973	0.0061	0.1348	0.0682
		0.2	0.9424	0.8956	6.2554	0.8309	5.9123	0.0053	0.1213	0.0662
		0.3	0.9423	0.8956	6.2286	0.8314	5.9299	0.0046	0.1070	0.0655
		0.4	0.9407	0.8928	6.0504	0.8276	5.8018	0.0040	0.0918	0.0666
	100	0.1	0.9446	0.8994	6.4969	0.8359	6.0936	0.0059	0.1374	0.0645
		0.2	0.9492	0.9086	7.0456	0.8497	6.6546	0.0049	0.1267	0.0581
		0.3	0.9539	0.9177	7.7078	0.8636	7.3306	0.0040	0.1151	0.0518
		0.4	0.9586	0.9269	8.5114	0.8773	8.1506	0.0031	0.1028	0.0459
	1000	0.1	0.9449	0.9000	6.5308	0.8367	6.1252	0.0059	0.1377	0.0642
		0.2	0.9499	0.9099	7.1379	0.8517	6.7414	0.0049	0.1272	0.0573
		0.3	0.9551	0.9200	7.9032	0.8669	7.5157	0.0039	0.1160	0.0504
		0.4	0.9604	0.9305	8.8967	0.8826	8.5182	0.0030	0.1040	0.0437

contribution to the energy integral through the term of increasing internal energy prevail upon that of the kinetic energy which is less altered. It is noted that in this case the influence of intensive heat flux, which is typical of isothermal flow condition, reduces markedly the level of the almost linearly running curves. Fig. 4 gives the results for the case $n = 1$ in which for $G = 1$ the energy integral decreases. The variations of J with k_p for different parameter G at $y = 0$ and $y = 0.01$ are shown in Fig. 3. It appears to have the same tendency as the previous cases. This is in accordance with the variation of both $f_p = \alpha$ and g_p which on basis of Eq. (33) mainly contributes to the energy integral. On the one hand, J changes with α to the power of $j + 1$. On the other hand, an enlargement of the work done by the piston (Eq. (31)), appears when g_p takes on higher values as can be seen from Tables 1 and 2. Moreover, the variations of both f_p and g_p with G at constant k_p are distinct for values of G up to 10 and approach to a maximum for $G = \infty$. This statement is valid for all values of n listed in the tables.

The distributions of the non-dimensional particle velocity, u/u_n, gas pressure, p/p_n, density, ϱ/ϱ_n, and heat flux, q/q_n for various dust parameters are given on Figs. 5–7. These figures illustrate the cases $n = -0.5$, $n = 1$, $n = 0$ and $y = 0$, $n = 0$ and $y = 0.01$. The effects of the volume fraction of the particles and the density ratio of the solid particles to the initial-gas G on the ratio $r_p/r_n = x_p$ are also shown in these figures. From these figures as well as from the tables one can find that this ratio decreases as k_p increases for $G = 1$ while it increases as k_p increases for $G \geqslant 10$. This means that the shock-front radius $r_n(t)$, as well as the shock-propagation velocity W_n, becomes larger with increasing k_p for $G = 1$ or smaller for $G \geqslant 10$, when one considers a given piston radius $r_p(t)$ at the same time t. Finally, the deviation of the isothermal flow field between the shock and the moving piston due to the presence of dust from that without small solid particles (perfect gas) becomes larger for $G = 1$ and smaller for $G \geqslant 10$.

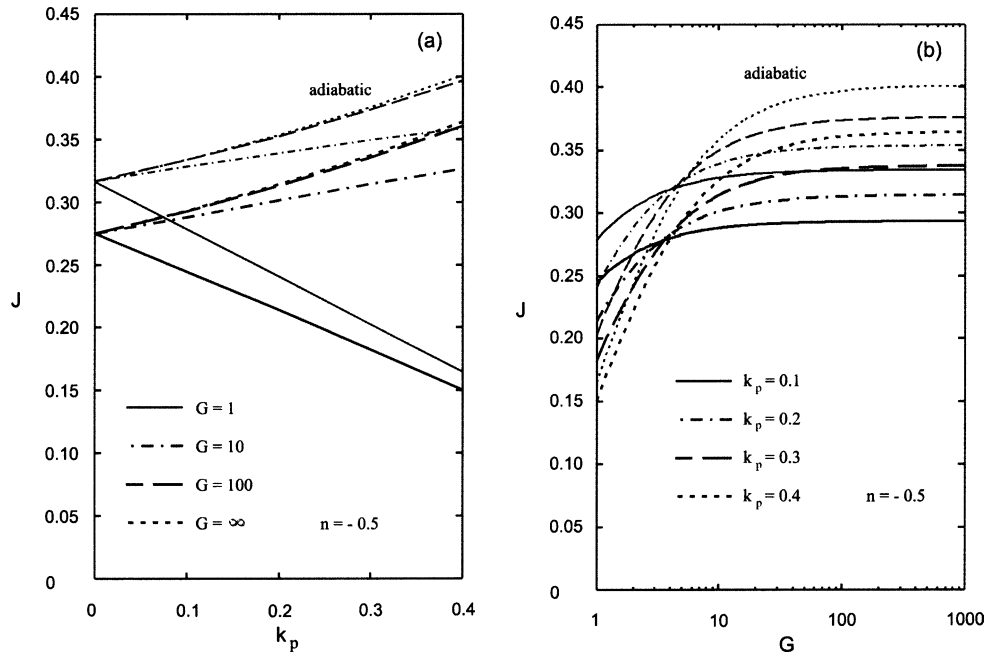

Fig. 2. Comparison of non-dimensional energy integral for spherical flow of a dust-laden gas under isothermal condition at $n = -0.5$ with that of adiabatic condition, presented in (a) versus k_p for different G, and in (b) versus G for different k_p.

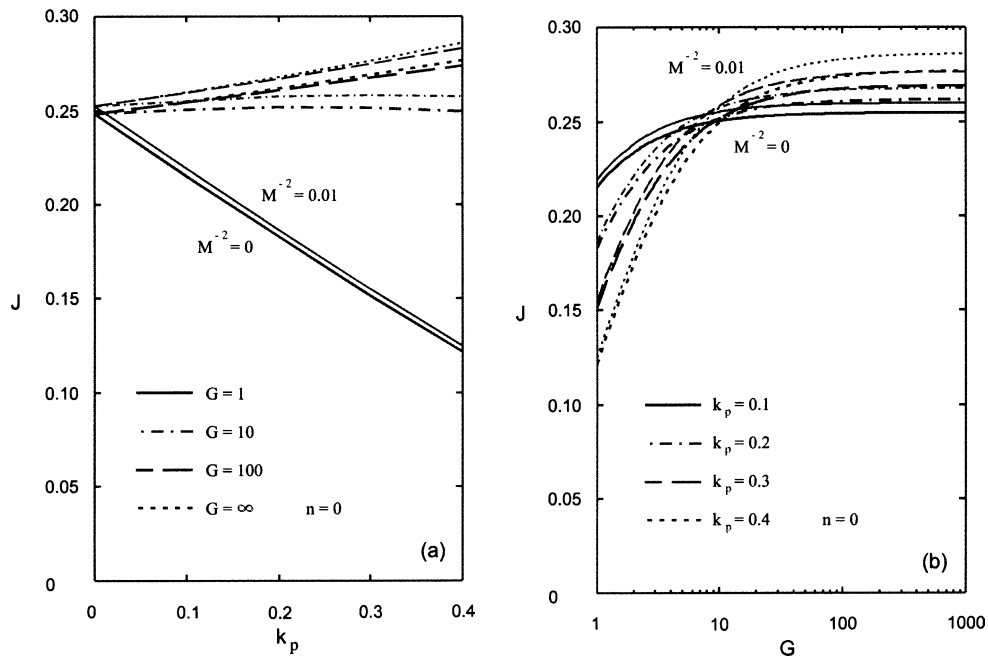

Fig. 3. Non-dimensional energy integral for spherical flow of a dust-laden gas under isothermal condition at $n = 0$ for different M^{-2}, presented in (a) versus k_p for different G, and in (b) versus G for different k_p.

The integral curves in the (Y, F)-plane are shown in Figs. 8–10 for different values of the dust parameters k_p and G. All the curves start from the Rankine–Hugoniot curve and have finite values at $F = 1$ corresponding to $h > 0$ which is different from the adiabatic case where $h = 0$. It is seen that the loci of the singularities, Eq. (38), do not intersect with any of the integral curves, i.e., the solutions are singularity free as already mentioned. Of course, all the integral curves are drawn with the correct λ

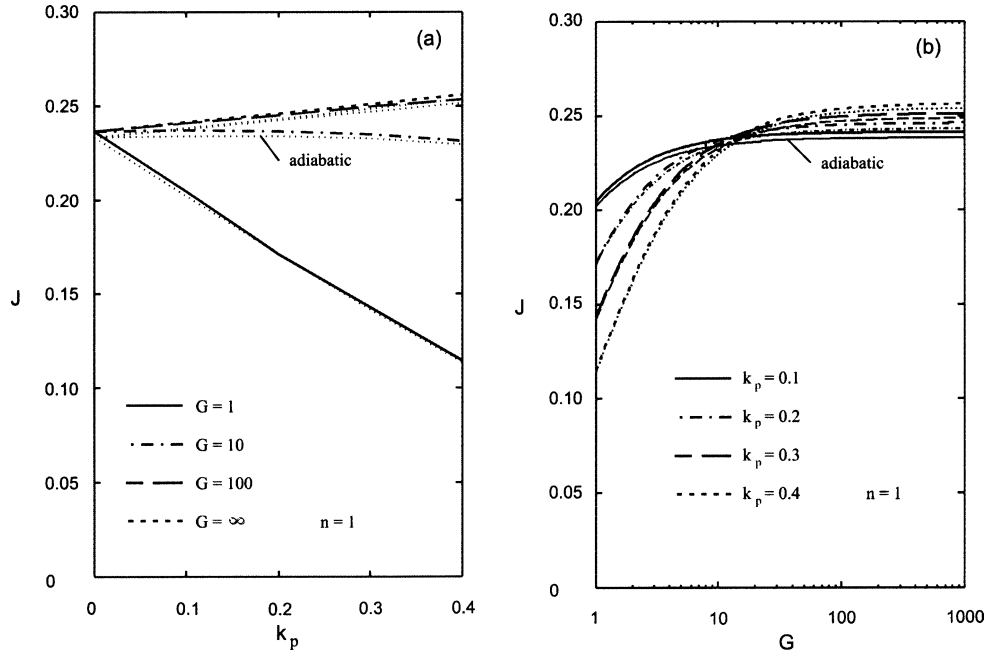

Fig. 4. Comparison of non-dimensional energy integral for spherical flow of a dust-laden gas under isothermal condition at $n = 1$ with that of adiabatic condition, presented in (a) versus k_p for different G, and in (b) versus G for different k_p.

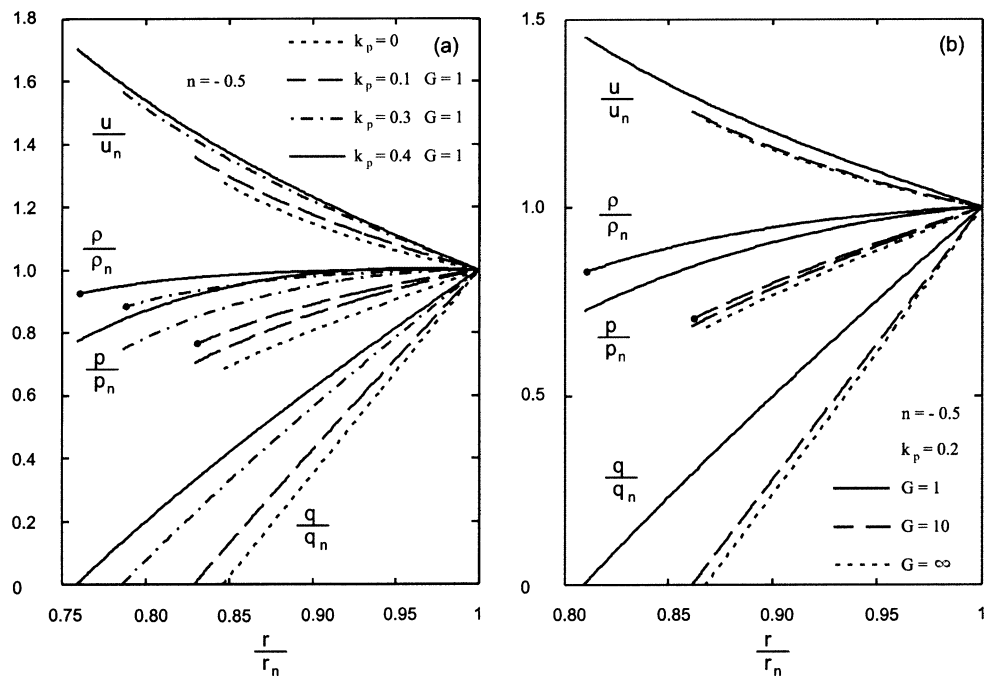

Fig. 5. Non-dimensional velocity u/u_n, pressure p/p_n, density ϱ/ϱ_n and heat flux q/q_n versus r/r_n for spherical flow of a dust-laden gas under isothermal condition at $n = -0.5$, presented in (a) for three different values of $k_p > 0$ and one constant value of G, and in (b) for one constant value of k_p and three different values of G. The pointed lines in (a) represent the dust-free case $k_p = 0$ and $G = 0$.

satisfying boundary conditions. Note that in the case $n = -0.5$ some of the integral curves have a maximum corresponding, for example, to $G = 1$ and $k_p \geqslant 0.2$.

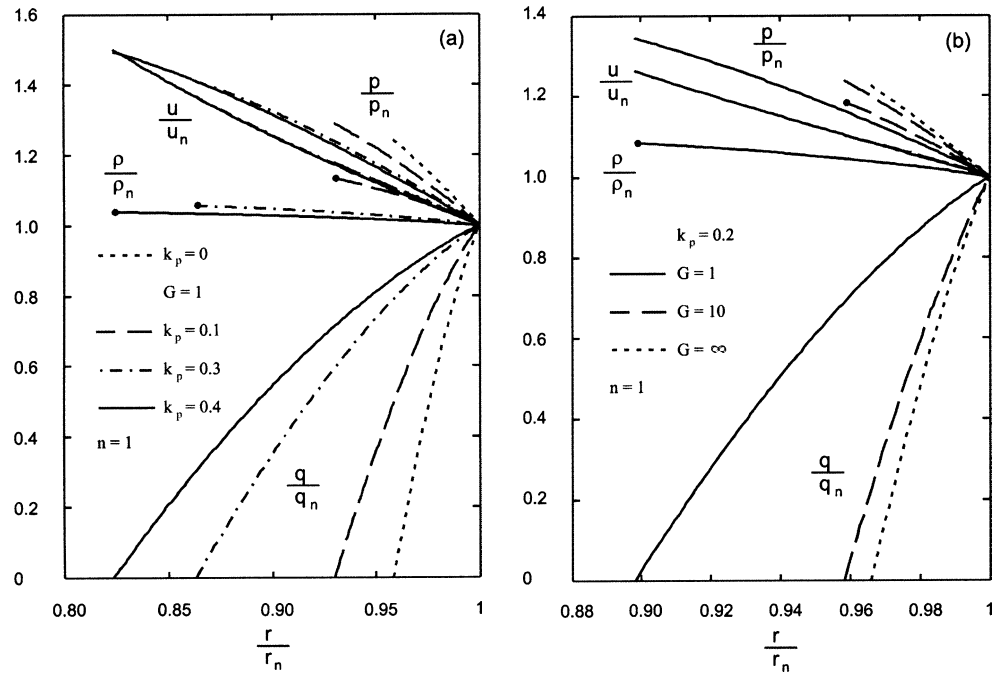

Fig. 6. Non-dimensional velocity u/u_n, pressure p/p_n, density ϱ/ϱ_n and heat flux q/q_n versus r/r_n for spherical flow of a dust-laden gas under isothermal condition at $n = 1$, presented in (a) for three different values of $k_p > 0$ and one constant value of G, and in (b) for one constant value of k_p and three different values of G. The pointed lines in (a) represent the dust-free case $k_p = 0$ and $G = 0$.

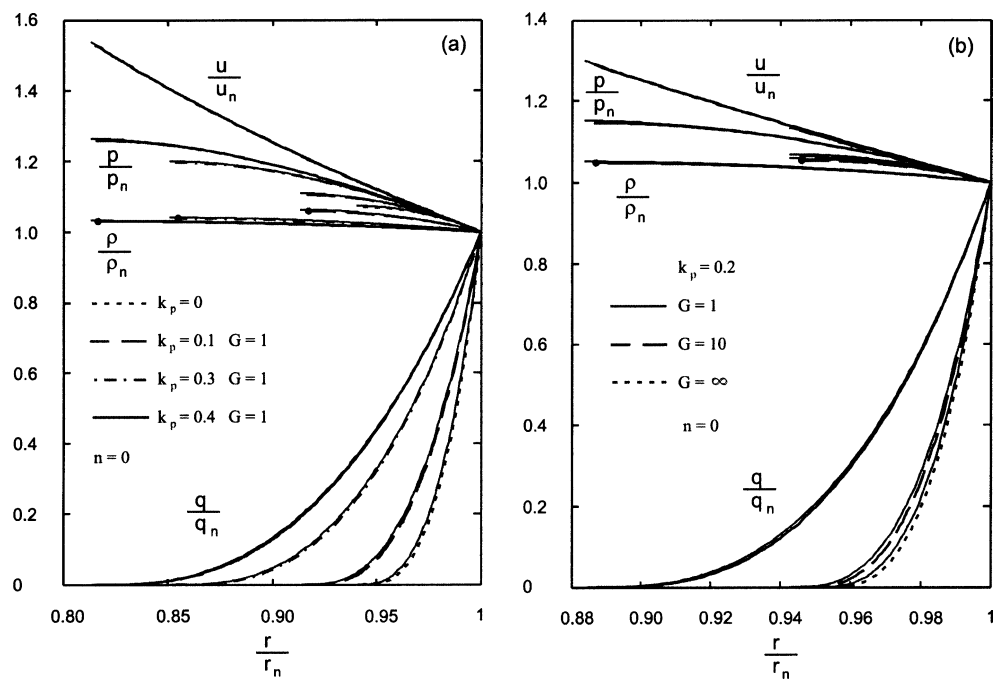

Fig. 7. Non-dimensional velocity u/u_n, pressure p/p_n, density ϱ/ϱ_n and heat flux q/q_n versus r/r_n for spherical flow of a dust-laden gas under isothermal condition at $n = 0$ and $y = 0$, presented in (a) for three different values of $k_p > 0$ and one constant value of G, and in (b) for one constant value of k_p and three different values of G. The pointed lines in (a) represent the dust-free case $k_p = 0$ and $G = 0$, while the thin lines in (a) and (b) represent the case $y = 0.01$.

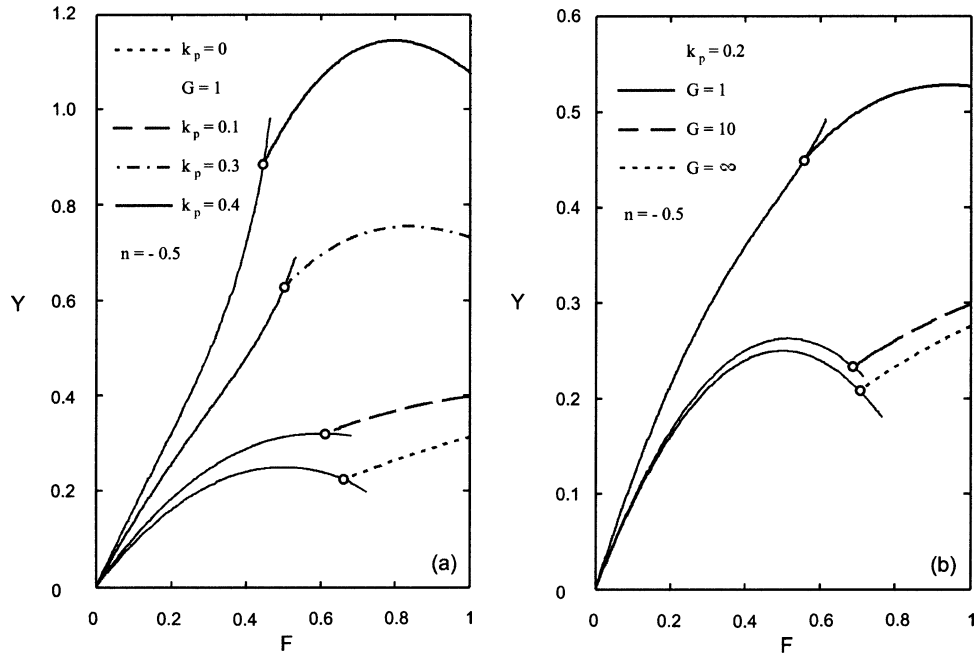

Fig. 8. The integral curve in the phase plane for spherical flow of a dust-laden gas under isothermal condition at $n = -0.5$ presented in (a) for three different values of $k_p > 0$ and one constant value of G, and in (b) for one constant value of k_p and three different values of G. The pointed lines in (a) represent the dust-free case $k_p = 0$ and $G = 0$.

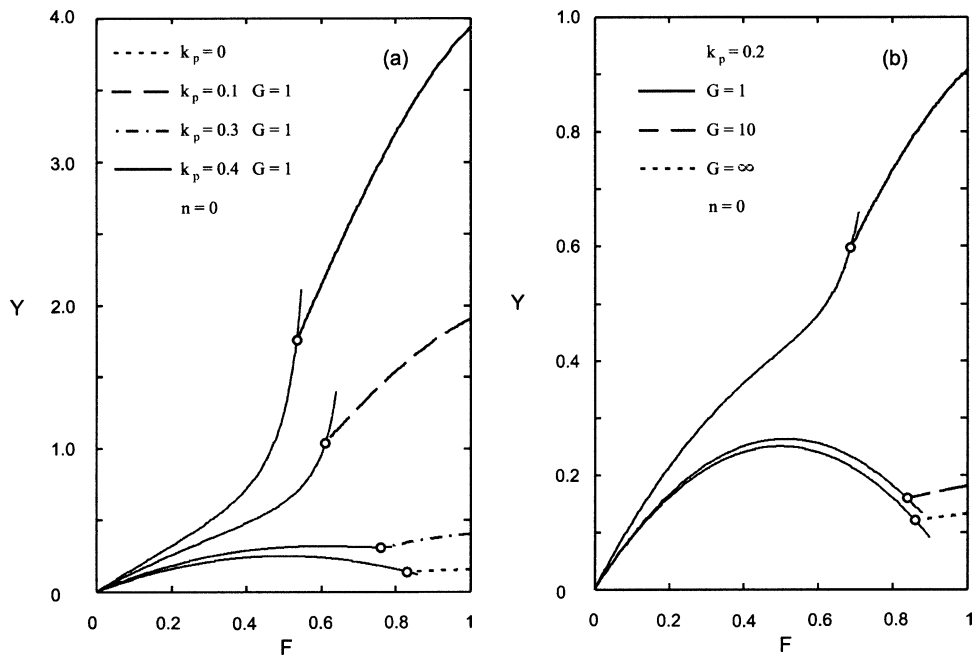

Fig. 9. The integral curve in the phase plane for spherical flow of a dust-laden gas under isothermal condition at $n = 0$ and $y = 0$ presented in (a) for three different values of $k_p > 0$ and one constant value of G, and in (b) for one constant value of k_p and three different values of G. The pointed lines in (a) represent the dust-free case $k_p = 0$ and $G = 0$.

According to the definition of Y, the local speeds of isothermal sound (i.e. a^2_{isoth}/W_n^2) are given by the points on the Rankine–Hugoniot curve. All three cases have the same characteristic: The isothermal sound speed increases as k_p increases

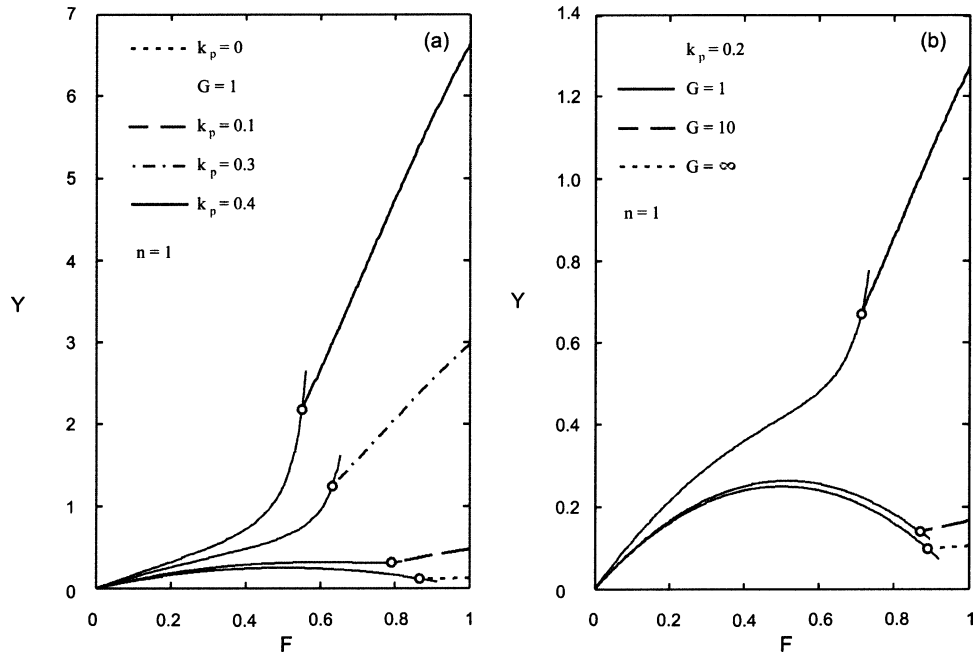

Fig. 10. The integral curve in the phase plane for spherical flow of a dust-laden gas under isothermal condition at $n = 1$ presented in (a) for three different values of $k_p > 0$ and one constant value of G, and in (b) for one constant value of k_p and three different values of G. The pointed lines in (a) represent the dust-free case $k_p = 0$ and $G = 0$.

for $G = 1$ and decreases as G increases for constant k_p, respectively. On the other hand, the isothermal speed of sound in the mixture is related to the isothermal compressibility, given by Eq. (7), which becomes lower with the dust load. The density ϱ decreases with higher values of k_p for $G = 1$ and increases with higher values of G, respectively, as shown for h_p and h_n in Tables 1 and 2.

4. Conclusion

Self-similar solutions for shock-wave propagation in a dust-laden gas of variable energy at very intensive heat exchange between gas particles have been presented. The total energy has been supplied by a driving piston according to a power law whose index β as well as the piston-velocity exponent n are quantities related linearly to the shock-front parameter λ characterizing the curvature of the front path in the time space domain. Applying the similarity requirements, the governing equations result in a boundary value problem consisting of three ordinary differential equations in which the dimensionless temperature Θ appears as a constant parameter.

Finally, it turns out that no energy outflow or inflow is necessary for this process to be realized. Since the shock front is opaque no loss due to radiation energy occurs. The conservation law holds on the shock front and is satisfied in the whole space. Therefore, when both β and α goes to zero the solution of the point explosion problems (Korobeinikov [3], Gretler and Regenfelder [12]) are limiting cases for the presented solution.

References

[1] K. Wang, The piston problem with thermal radiation, J. Fluid Mech. 20 (1964) 447–455.
[2] J.B. Helliwell, Self-similar piston problems with radiative heat transfer, J. Fluid Mech. 37 (1968) 497–512.
[3] V.P. Korobeinikov, Problems in the theory of point explosion in gases, Proc. Steklov Inst. Math. 119 (1973) (Am. Math. Soc. 1976, Providence, RI).
[4] D.D. Laumbach, R.F. Probstein, A point explosion in a cold exponential atmosphere, J. Fluid Mech. 35 (1969) 53–75.
[5] G. Narasimhulu Naidu, M.P. Ranga Rao, Yadav, Astrophs. Space Si. 89 (1983) 77.
[6] V.A. Levin, T.A. Zhuravskaya, Propagation of converging and diverging shock waves under isothermal condition, Shock Waves 6 (1996) 177–182.

[7] G. Narasimhulu Naidu, K. Venkatanandam, M.P. Ranga Rao, Approximate analytical solutions for self-similar flows of a dusty gas with variable energy, Int. J. Engrg. Sci. 23 (1) (1985) 39–49.
[8] W. Gretler, R. Regenfelder, Similarity solution for laser-driven shock waves in a dust-laden gas with internal heat transfer effects, Fluid Dyn. Res. 30 (2002) 239–313.
[9] S.I. Pai, S. Menon, Z.Q. Fan, Similarity solution of a strong shock wave propagation in a mixture of gas and dusty particles, Int. J. Engrg. Sci. 18 (1980) 1365–1373.
[10] J.H. Geng, H. Groenig, Dust suspensions accelerated by shock waves, Experiment. Fluids 28 (2000) 360–367.
[11] R.A. Freeman, Variable energy blast wave, J. Phys. D 1 (1968) 1697–1710.
[12] W. Gretler, R. Regenfelder, Similarity solution for variable energy shock waves in a dusty gas under isothermal condition, Fluid Dyn. Res. 32 (2003) 69–84.